Technological advances on Si and Si3N4 low-loss waveguide platforms for nonlinear and quantum optics applications

Cyril Bellegarde, Houssein El Dirani, Xavier Letartre, Camille Petit-Etienne, Christelle Monat, Jean-Michel Hartmann, Corrado Sciancalepore, Erwine Pargon

PROCEEDINGS OF SPIE

SPIEDigitalLibrary.org/conference-proceedings-of-spie

Technological advances on Si and Si3N4 low-loss waveguide platforms for nonlinear and quantum optics applications

Cyril Bellegarde, Houssein El Dirani, Xavier Letartre, Camille Petit-Etienne, Christelle Monat, et al.

Cyril Bellegarde, Houssein El Dirani, Xavier Letartre, Camille Petit-Etienne, Christelle Monat, Jean-Michel Hartmann, Corrado Sciancalepore, Erwine Pargon, "Technological advances on Si and Si3N4 low-loss waveguide platforms for nonlinear and quantum optics applications," Proc. SPIE 10933, Advances in Photonics of Quantum Computing, Memory, and Communication XII, 1093309 (4 March 2019); doi: 10.1117/12.2508617

SPIE.

Event: SPIE OPTO, 2019, San Francisco, California, United States

Technological advances on Si and Si_3N_4 low-losses waveguide platforms for nonlinear and quantum optics applications

Cyril Bellegarde[2], Houssein El Dirani[1], Xavier Letartre[3], Camille Petit-Etienne[1], Christelle Monat[3]
Jean-Michel Hartmann[1], Corrado Sciancalepore[1] and Erwine Pargon[2]

[1]Univ. Grenoble Alpes, CEA-LETI, Minatec, Optics and Photonics Division, 17 rue des Martyrs, F-38054 Grenoble, France
[2] LTM, Centre National de la Recherche Scientifique, University Grenoble Alpes, 38000 Grenoble, France
[3]Institut des nanotechnologies de Lyon, UMR CNRS 5270, Ecole Centrale Lyon, Ecully, France

ABSTRACT

In this communication, we report on the design, fabrication, and testing of silicon-on-insulator (SOI) and silicon-nitride-on-insulator (SiNOI) photonic circuits for nonlinear and quantum optics applications. As recently demonstrated, the generation of correlated photons on Si platforms can be used for quantum cryptography and quantum computing. Concerning SiNOI waveguides, Kerr frequency combs have been proposed in many applications, such as atomic clocks, on-chip spectroscopy, and terabit coherent communications. Silicon is an attractive platforms for correlated photons sources because of its high nonlinearity, they can have several modes in telecom band with sharp line widths (tens of μeV) and its inherent complementary metal-oxide-semiconductor (CMOS) compatibility. Moreover, the SiNOI is an attractive platform for Kerr comb generation due to their large bandgap and consequently the low two-photon absorption in the telecommunication band. Furthermore, in all the previous SiNOI-based frequency combs, the silicon nitride film undergoes long and high-temperature annealing to reduce the absorption in the telecommunication band caused by the dangling N-H bonds, thus making such annealed Si_3N_4 films non-CMOS compatible. However, both in the case of correlated photons pairs generation and Kerr frequency combs, the source efficiency is related to the quality factor (Q), so that a high-Q resonator is required to get highly-efficient sources. Authors report here about the fabrication and the characterization of annealing-free CMOS-compatible SiNOI- and hydrogen-annealed silicon-based waveguides and microresonators featuring ultra-low losses (*e.g.,* 0.6 dB/cm for single-mode Si waveguides) that can be used, respectively, as efficient sources for Kerr combs and correlated photon pairs sources.

Keywords: Complementary metal-oxide-semiconductor (CMOS), nonlinear integrated optics, quantum integrated circuits, Kerr-based comb generation, resonators, photonic integrated circuits (PICs), silicon nitride (Si_3N_4), correlated photons, hydrogen annealing.

1. LOW-LOSS SILICON NITRIDE FOR NONLINEAR PHOTONICS

Kerr frequency combs constitute a paradigm shift in the development of high-capacity data transmission, integrated spectroscopy, high precision metrology, and frequency synthesis [1]. Since 2010, silicon-nitride-on-insulator (SiNOI) has imposed as an attractive chip-based platform for the generation of wideband frequency combs pumped at telecom wavelengths, because of its relatively high nonlinearity (×10 that of silica and larger than that of highly nonlinear Hydex glass [2]) as well as the absence of two-photon absorption and free carrier generation that plague crystalline silicon. In the meanwhile, silicon photonics integrated circuits (Si-PICs) have demonstrated increasing maturity levels for a wide range of optical functions such as III-V-on-Si integrated lasers [3], high-speed modulators [4], Ge-on-Si photodiodes [5], as well as filters and wavelength (de)multiplexers [6], thus continuously highlighting the potential of silicon optoelectronics integration with cost-effective complementary metal-oxide-semiconductor (CMOS) technology [7,8]. In this context, the monolithic co-integration of Kerr-based frequency combs with Si photonics holds the promise for on-chip high-capacity transmitters that would benefit from the maturity and low cost of CMOS manufacturing and scalability.

The realization of relatively thick (> 700 nm) stoichiometric Si3N4 films, as required by microring frequency combs, which imply both a tight confinement of light and anomalous group velocity dispersion (GVD), remains challenging. In

Advances in Photonics of Quantum Computing, Memory, and Communication XII, edited by
Philip R. Hemmer, Alan L. Migdall, Zameer Ul Hasan, Proc. of SPIE Vol. 10933, 1093309
 · doi: 10.1117/12.2508617

particular, all prior works strictly made use of long high-temperature annealing (~1200 °C for at least 3h) of the deposited silicon nitride film [9-12]. This extreme annealing step has been accounted for by the need to densify the silicon nitride film through driving out excess hydrogen and break N-H bonds, so as to get closer to a stoichiometric Si_3N_4 film and reduce the material absorption loss in the C-band. However, this annealing induces thermal stress that eventually leads to cracks during the device processing unless sophisticated pre-patterning strategies are adopted prior to the film deposition [10, 11]. Yet, in the context of nonlinear optics-silicon optoelectronics co-integration, these extreme annealing temperatures would severely degrade the front-end silicon optoelectronics circuit underneath. Specifically, doped optical circuits would be unacceptably affected by the undesirable dopant diffusion in junction-based Si modulators and by the hetero-interface degradation of Ge-on-Si photodetectors. Very recently, we reported a new method that avoids thermal annealing for realizing relatively thick (740 nm) crack-free Si_3N_4-based straight nanowaveguides with good linear and nonlinear properties measured by self-phase modulation [15]. Here, we report for the first time the realization of annealing-free silicon nitride comb microresonators, following a tailored deposition method which minimizes the hydrogen content. Our annealing-free and crack-free fabrication process (shown in Fig. 1) provides our devices with the right specification (microring GVD and characteristics) to underpin Kerr frequency combs, thus representing a significant step toward the full compatibility of Si_3N_4-based Kerr comb sources with the thermal budgets of Si photonics processing. In contrast to all previous approaches, our process does not exceed neither the dopant activation temperature (1030 °C) required for Si modulators [13], nor the H_2 annealing thermal budget used for dislocations control for Ge-on-Si photodiodes (825 °C) [14].

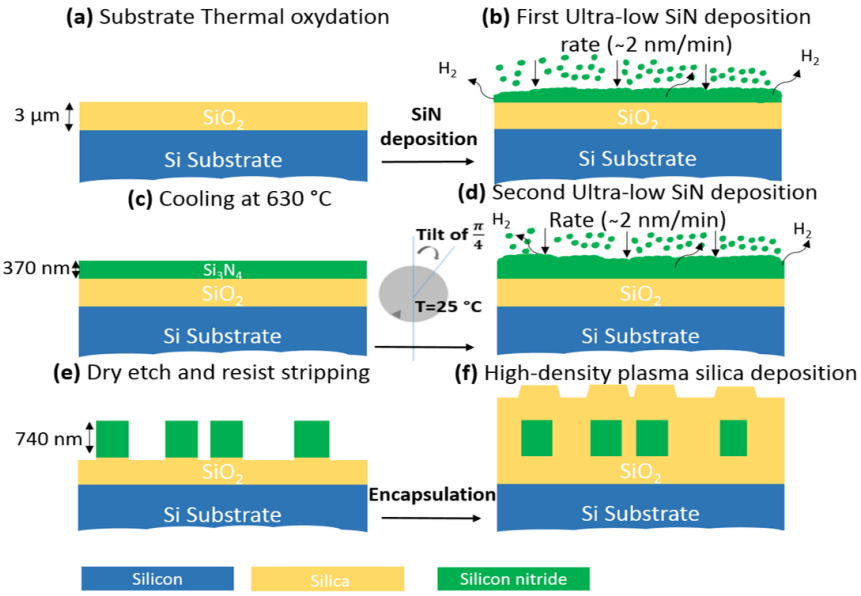

Fig. 1. Schematics of the annealing-free fabrication process for Si3N4 nonlinear photonics (a)-(f).

The measured spectrum of an annealing-free silicon-nitride-on-insulator microring with a 56-µm radius is shown in Fig. 2. A native line spacing frequency comb spanning across about 730 nm between 1340 nm - 2070 nm was measured when a continuous-wave pump power of ~ 1 W at 1569 nm– was coupled in the bus waveguide. The loaded quality factor of the ring resonator separated by a 350 nm gap from the bus waveguide exceeds 580,000 at the pump wavelength. The cross-section dimensions (1.5-µm-wide × 740-nm-thick) of the ring ensure that GVD is anomalous at the pump wavelength.

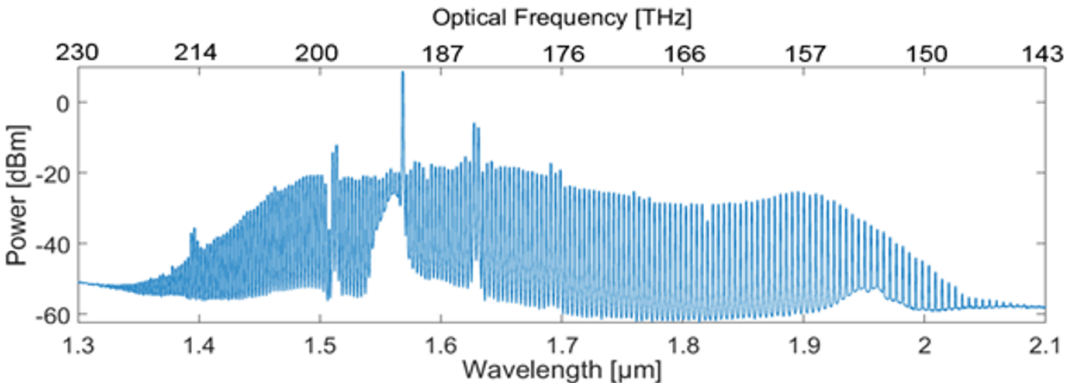

Fig. 2. Comb generation using annealing-free silicon nitride on insulator. A 730-nm-spanning comb generation using a 56-μm-radius Si3N4 microresonator.

Interestingly, a slight signature of residual hydrogen-related absorption can be observed in the comb around 1508 nm, but it remains comparable to previous works employing film annealing and does not hinder the generation of a relatively wide and flat comb spectrum. The difference between the losses at 1550 nm ($Q_i = 350{,}000$) and the losses at 1520 nm ($Q_i = 190{,}000$) can thus be estimated to be 0.9 dB/cm. This additional loss due to residual N-H absorption for our annealing-free process is comparable to the value (0.6 dB/cm) inferred for high-temperature annealed Si_3N_4 waveguides [16], and, as shown above, it does not preclude the parametric oscillation and comb generation in the C-band.

In conclusion, generating a wideband comb at telecom wavelengths using annealing-free silicon nitride nonlinear circuits featuring a full FEOL process compatibility with Si photonics is possible [17]. Via such demonstration, we claim the *first-time realization* of annealing-free silicon nitride frequency comb microresonators, following a tailored deposition method, minimizing the hydrogen content. The right specification (microring group velocity dispersion and characteristics) are provided by our annealing-free and crack-free fabrication process to underpin Kerr frequency combs, thus representing a significant step toward the full compatibility of Si_3N_4-based Kerr-comb sources monolithic integration with standard CMOS and Si photonics processing. Through allowing the monolithic integration of broadband comb sources with CMOS-compatible optoelectronics, our work represents a milestone toward the realization of next-generation Petabit/s data transmitters on a chip.

2. ULTRA-LOW LOSS SILICON PHOTONICS CIRCUITS FOR QUANTUM APPLICATIONS

In previous publications [18], [19], we reported that the introduction of a high-temperature hydrogen annealing (> 800 ° C) after the silicon waveguide etching was particularly effective to decrease the silicon sidewalls roughness and consequently reduce the optical losses. However, this annealing leads also to a pattern deformation which depends on the shape of the guide and the interfaces. Indeed, the surface migration of silicon atoms activated by the H_2 annealing evolves towards a surface energy-minimizing configuration, while the total volume is preserved. The consequence is that the right angles of the pattern tend to round off. Typically, in the case of STRIP guides, the deformation is limited by the Si / SiO_2 BOX interface at the bottom of the pattern, which is no longer the case for the RIB guides. Figure 3 illustrates the STRIP and RIB waveguide deformations occurring with our standard H_2 annealing conditions (850 °C/20 Torr /2 min.). In this example, the Si waveguides are patterned with a resist mask that is removed before the annealing treatment. For both STRIP and RIB, the pattern height and volume are not modified by the annealing, while top corners round. In the STRIP case, the bottom CD is reduced of about 30 nm while the middle CD is enlarged of about 20 nm, which is acceptable In the RIB case, a severe enlargement of the bottom CD is observed in the RIB case, which is an acceptable pattern dimension variation. In the RIB case, the bottom CD is significantly increased of 170 nm, which is not tolerable for the circuitry design.

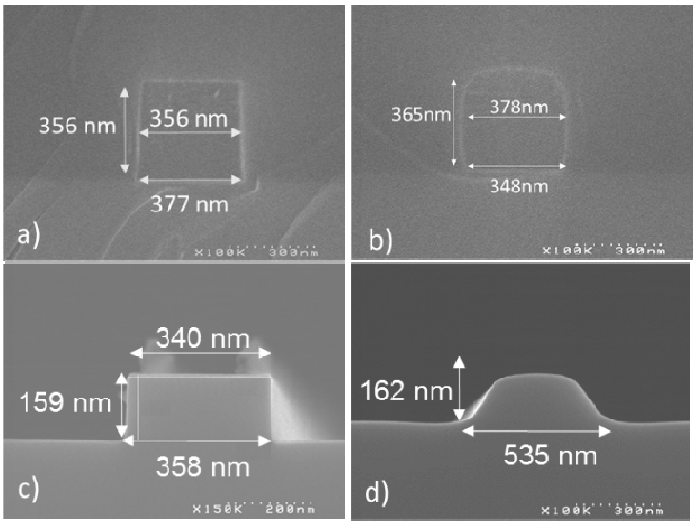

Fig. 3. SEM-cross section images of STRIP ((a) and (b)) and RIB ((c) and (d)) waveguides profiles after patterning without ((a) and (c)) and with ((b) and (d)) H_2 annealing using 850°C/20Torr during 2 min.

The sidewalls roughness of the STRIP and RIB waveguides is evaluated by AFM before and after H_2 annealing using the standard conditions (cf. Fig. 4). With this technique, the line edge roughness (LER) can be estimated all along the pattern height and an average LER can be calculated. Before annealing, both RIB and STRIP have similar average LER of 1.8 nm. After annealing, the line edge of roughness of the pattern are significantly decreased of 55% and 78% for STRIP and RIB respectively. As expected, the roughness reduction is much more important in the RIB case since no Si/SiO_2 interface limits the atomic surface migration but it is at a cost of profile loss.

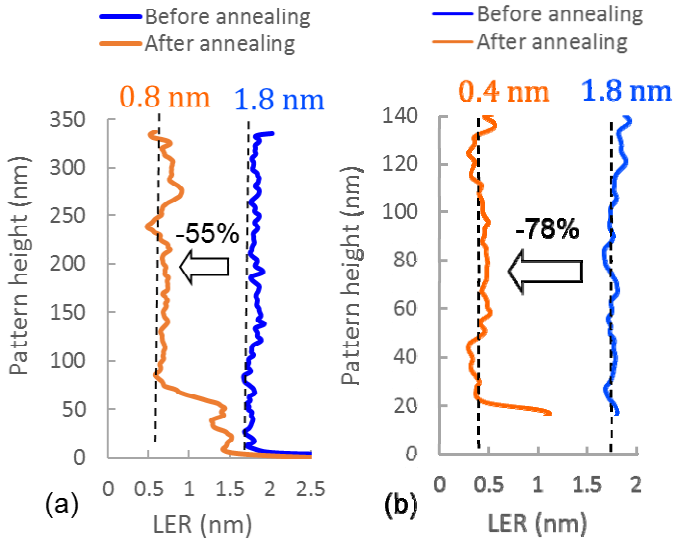

Fig. 4: Line edge roughness (LER) measured by AFM along the Si waveguide height before and after H_2 annealing (850°C/20Torr/2min): a) STRIP case, b) RIB case

There is therefore a trade-off between reducing the roughness and preserving the shape of the guides.
In this work, we optimize the annealing conditions so that they are compatible with all types of waveguide architecture integrated in the passive circuit of the photonic circuit. As already reported [19], three key parameters drive the annealing process: temperature, time and pressure. An increase in temperature or annealing time, as well as a decrease

in hydrogen pressure favor the atomic surface migration. To obtain optimal annealing conditions adapted to any types of guide structure (STRIP, RIB, Deep RIB), it is necessary either to favor short times for aggressive conditions of pressure and temperature, or long times for milder conditions in temperature and pressure.

After H_2 annealing optimization, the enlargement of the RIB bottom dimension is only of 50 nm while the average LER is still of 0.43nm as for our standard more aggressive conditions (cf. Fig. 5). Concerning, the STRIP, the profile with the optimized conditions is similar to the one obtained with the standard conditions. However, it seems that the roughness degradation that can be observed at the bottom of the pattern with the standard condition (cf. Fig 6a) is reduced with the optimized conditions. The AFM measurement shown in Fig 6c indicates that with the optimized H_2 annealing conditions, the LER of the top and middle sidewalls is higher than for the standard conditions (1.06 nm vs 0.7nm). But they confirm that the LER at the pattern bottom is greatly improved from 1.85nm to 0.76nm with the optimized conditions. Figure 7 shows the optical losses measured at 1310nm for STRIP and RIB patterned without and with the optimized H_2 annealing conditions. It clearly demonstrates the beneficial impact of H_2 annealing on optical losses that are reduced of more than 70% for both RIB and STRIP. Record loss values of less than 1.1dB/cm and less than 0.34 dB/cm are obtained for STRIP and RIB waveguides, whatever their width. Although the average STRIP sidewalls roughness is higher with the optimized conditions, the optical losses of the STRIP waveguides are as low as with our standard conditions and even better for the smaller waveguide CDs. This suggests that the roughness degradation at the pattern bottom which is higher for the standard conditions has a disastrous impact on the optical losses especially for small waveguides.

In this work, we proposed optimized H_2 annealing conditions that allow to smooth RIB and STRIP waveguide sidewalls while keeping satisfying profile and dimensions. The use of this optimized treatment allowed us to fabricate ultra-low loss RIB and STRIP waveguides with loss values at the best of the state of the art.

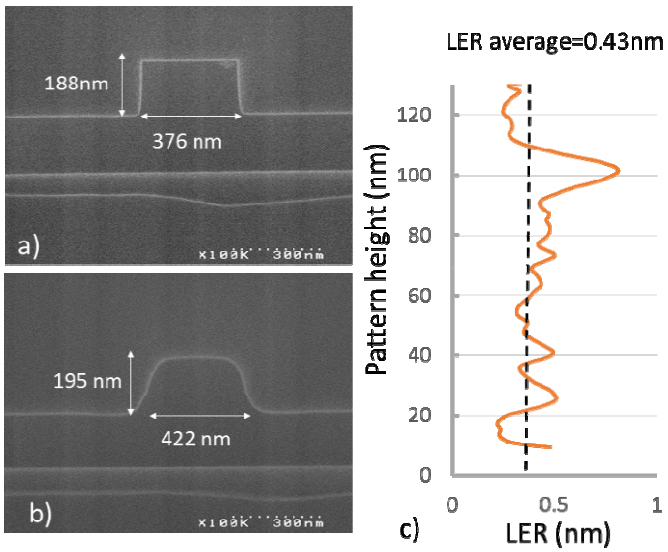

Fig. 5. SEM cross section images of the RIB waveguide profiles after encapsulation without (a) and (b) with the optimized H_2 annealing treatment; c) Line edge roughness measured by AFM along the RIB waveguide sidewalls after etching and optimized H_2 annealing conditions.

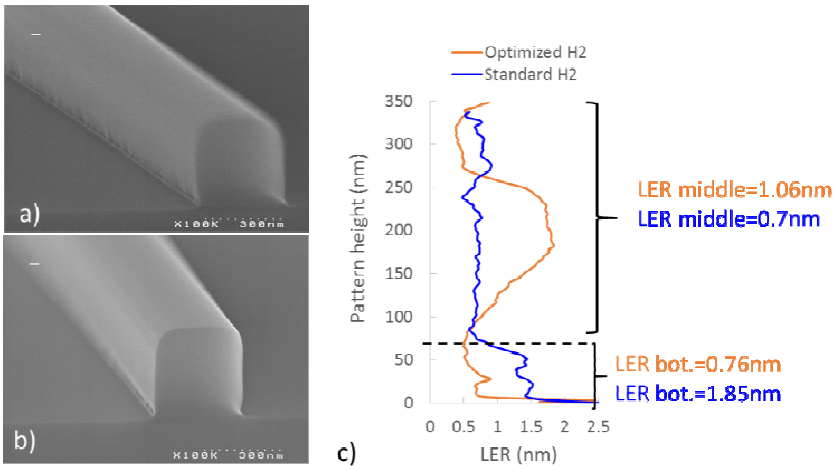

Fig. 6: a) Tilted SEM cross section images of the STRIP waveguide profiles after a) standard and b) optimized H_2 annealing; c) Line edge roughness measured by AFM along the STRIP sidewalls after the standard and optimized H_2 annealing treatment.

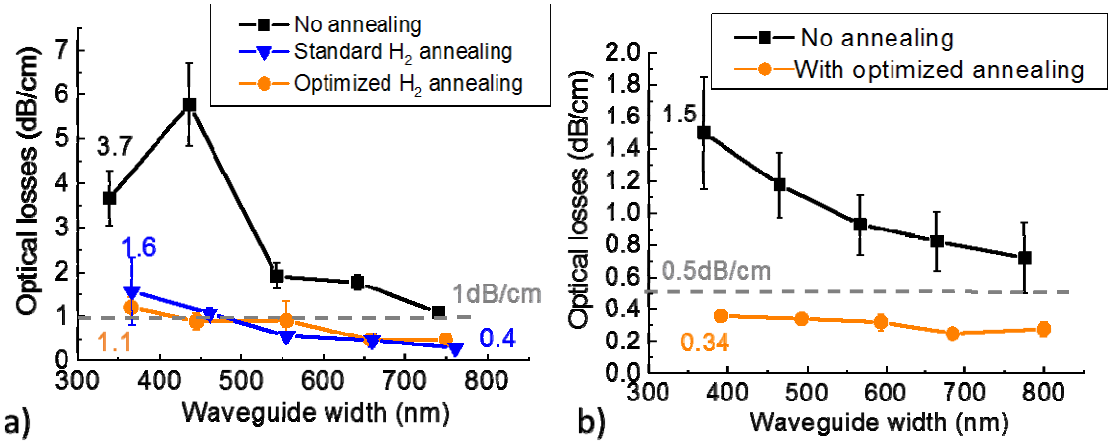

Fig. 7. Optical losses measured at 1310nm as a function of the waveguide width for a) STRIP and b) RIB patterned without and with the optimized H_2 annealing. The optical results for the standard H_2 annealing conditions are also represented in the STRIP case.

FUNDING

DOPT 2020 internal funding program and the IRT Nanoelec (CEA-LETI and LTM). Danish Research Council SPOC (DNRF-123) center of excellence silicon photonics for communications (SPOC) (DTU). ERC H2020 GRAPHICS (648546) and the Institut Universitaire de France (INL).

REFERENCES

[1] Marin-Palomo, P., Kemal, J. N., Karpov, M., Kordts, A., Pfeifle, J., Pfeiffer, M. H. and Rosenberger, R., "Microresonator-based solitons for massively parallel coherent optical communications," Nat. Papers 546(7657), 274 (2017).

[2] Moss, D. J., Morandotti, R., Gaeta, A. L. and Lipson, M., "New CMOS-compatible platforms based on silicon nitride and Hydex for nonlinear optics,'' Nat. Phot. Papers 7(8), 597 (2013).

[3] Bakir, B. B., Descos, A., Olivier, N., Bordel, D., Grosse, P., Augendre, E. and Fedeli, J. M., "Electrically driven hybrid Si/III-V Fabry-Pérot lasers based on adiabatic mode transformers,'' Opt. Exp. Papers 19(11), 10317-10325 (2011).

[4] Liao, L., Samara-Rubio, D., Morse, M., Liu, A., Hodge, D., Rubin, D. and Franck, T., "High speed silicon Mach-Zehnder modulator,'' Opt. Exp. Papers 13(8), 3129-3135 (2005).

[5] Vivien, L., Rouvière, M., Fédéli, J. M., Marris-Morini, D., Damlencourt, J. F., Mangeney, J. and Pascal, D., "High speed and high responsivity germanium photodetector integrated in a Silicon-On-Insulator microwaveguide,'' Opt. Exp. Papers 15(15), 9843-9848 (2007).

[6] Bogaerts, W., Selvaraja, S. K., Dumon, P., Brouckaert, J., De Vos, K., Van Thourhout, D. and Baets, R., "Silicon-on-insulator spectral filters fabricated with CMOS technology,'' IEEE. J. Sel. Topics in quant. Elec., Papers 16(1), 33-44 (2010).

[7] Reed, G. T., "Device physics: the optical age of silicon,'' Nat. Papers 427(6975), 595 (2004).

[8] Asghari, M. and Krishnamoorthy, A. V., "Silicon photonics: Energy-efficient communication," Nat. Phot. Papers 5(5), 268 (2011).

[9] Levy, J. S., Gondarenko, A., Foster, M. A., Turner-Foster, A. C., Gaeta, A. L. and Lipson, M., "CMOS-compatible multiple-wavelength oscillator for on-chip optical interconnects,'' Nat. Phot. Papers 4(1), 37 (2010).

[10] Luke, K., Dutt, A., Poitras, C. B. and Lipson, M., "Overcoming Si3N4 film stress limitations for high quality factor ring resonators,'' Opt. Exp. Papers 21(19), 22829-22833 (2013).

[11] Pfeiffer, M. H., Kordts, A., Brasch, V., Zervas, M., Geiselmann, M., Jost, J. D. and Kippenberg, T. J., "Photonic Damascene process for integrated high-Q microresonator based nonlinear photonics,'' Optica, Papers 3(1), 20-25 (2016).

[12] Kim, S., Han, K., Wang, C., Jaramillo-Villegas, J. A., Xue, X., Bao, C. and Qi, M., "Dispersion engineering and frequency comb generation in thin silicon nitride concentric microresonators ," Nat. Com. Papers 8(1), 372 (2017).

[13] Streshinsky, M., Ding, R., Liu, Y., Novack, A., Yang, Y., Ma, Y. and Baehr-Jones, T., " Low power 50 Gb/s silicon traveling wave Mach-Zehnder modulator near 1300 nm ," Opt. Exp. Papers 21(25), 30350-30357 (2013).

[14] Michel, J., Liu, J. and Kimerling, L. C. "High-performance Ge-on-Si photodetectors," Nat. Phot. Papers 4(8), 527 (2010).

[15] El Dirani, H., Casale, M., Kerdiles, S., Socquet-Clerc, C., Letartre, X., Monat, C. and Sciancalepore, C., "Crack-Free Silicon-Nitride-on-Insulator Nonlinear Circuits for Continuum Generation in the C-Band," IEEE Phot. Tech. Lett. Papers 30(4), 355-358 (2018).

[16] Krückel, C. J., Fülöp, A., Ye, Z. and Andrekson, P. A., " Optical bandgap engineering in nonlinear silicon nitride waveguides,'' Opt. Exp. Papers 25(13), 15370-15380 (2017).

[17] El Dirani, H., Kamel, A., Casale, M., Kerdiles, S., Monat, C., Letartre, X. and Sciancalepore, C. "Annealing-free Si3N4 frequency combs for monolithic integration with Si photonics," Appl. Phys. Lett. Papers 113(8), 081102-081105 (2018).

[18] C. Bellegarde, E. Pargon, C. Sciancalepore, C. Petit-Etienne, V. Hughes, D. Robin-Brosse, J-M Hartmann, P. Lyan, “Improvement of Sidewall Roughness of Sub-Micron SOI Waveguides by Hydrogen Plasma and Annealing”,IEEE Photonic Techno. Letter 30, (7) 591-594 (2018)

[19] C. Bellegarde, E. Pargon, C. Sciancalepore, C. Petit-Etienne, O. Lemmonier, K. Ribaud, J-M Hartmann, P. Lyan, Optimization of H_2 thermal annealing process for the fabrication of ultra-low loss sub-micron silicon-on-insulator rib waveguides, Proc. SPIE 10537, Silicon Photonics XIII, 1053706 (2018);